Research Square

Preprints are preliminary reports that have not undergone peer review.
They should not be considered conclusive, used to inform clinical practice,
or referenced by the media as validated information.

Genome analysis and cellulose production of Komagataeibacter oboediens GUS3

Banu Metin

banu.metin@yildiz.edu.tr

Yıldız Technical University

Hümeyra Odabaş

Istanbul Sabahattin Zaim University

Research Article

Keywords: Bacterial cellulose, Komagataeibacter oboediens, cellulose biosynthesis, bcs operons, whole-genome sequencing, carbon source utilization

Posted Date: November 24th, 2026

DOI: https://doi.org/10.21203/rs.3.rs-11728304/v1

License: This work is licensed under a Creative Commons Attribution 4.0 International License.
Read Full License

Additional Declarations: No competing interests reported.

Genome analysis and cellulose production of *Komagataeibacter oboediens* GUS3

Banu Metin*[1,2], Hümeyra Odabaş[2]

[1] Department of Food Engineering, Faculty of Chemical and Metallurgical Engineering, Yildiz Technical University, 34210 Istanbul, Türkiye

[2] Department of Food Engineering, Faculty of Engineering and Natural Sciences, Istanbul Sabahattin Zaim University, 34303 Istanbul, Türkiye

ORCID

Banu Metin: 0000-0002-3203-0058

Hümeyra Odabaş: 0000-0003-4815-9507

*Corresponding author

E-mail address: banu.metin@yildiz.edu.tr (B. Metin)

Author contributions

Banu Metin: Conceptualization, Methodology, Investigation, Supervision, Project administration, Funding acquisition, Writing - review & editing.

Hümeyra Odabaş: Methodology, Investigation, Formal analysis, Data curation, Visualization, Writing – original draft.

Funding

This work was supported by Istanbul Sabahattin Zaim University under Grant No. BAP-1000-42 awarded to B.M.

Abstract

Bacterial cellulose (BC) is a biopolymer valued for its purity, nanofibrillar structure, and water-holding capacity. This study integrated genomic characterization of a BC-producing strain, GUS3, isolated from homemade grape vinegar, with evaluation of cultivation conditions and BC properties. Illumina sequencing yielded a 3.6-Mb draft genome containing 3,387 predicted genes. Average nucleotide identity (97.99%) and digital DNA–DNA hybridization (86.6%) with *Komagataeibacter oboediens* LMG 18849^{T} supported identification as *K. oboediens*. Four cellulose biosynthesis (*bcs*) gene clusters were identified, including the canonical *bcsABCD* cluster and three clusters containing fused *bcsAB* genes. BC production was evaluated in HS medium using a one-factor-at-a-time approach across initial pH 3.0–9.0 and temperatures of 24–38 °C. At pH 6.5 and 32 °C, wet and dry BC yields reached 223.7 and 1.34 g/L, respectively. Glucose and fructose supported BC production, whereas lactose, sucrose, and glycerol did not support growth or BC production. Despite genomic assignments for enzymes potentially involved in sucrose and glycerol metabolism, neither substrate supported growth. Supplementation with 1% corn oil significantly increased wet BC weight, whereas 1–2% sunflower oil significantly increased dry BC weight relative to the control. The resulting BC showed characteristic FTIR bands, a homogeneous nanofibrillar network with fiber diameters of 29–55 nm, and a water-holding capacity of 99.3%. These findings connect genomic potential with observed substrate utilization and demonstrate cultivation-dependent differences in wet and dry BC production, providing a basis for further development of GUS3-based BC processes.

Keywords: Bacterial cellulose; *Komagataeibacter oboediens*; cellulose biosynthesis; *bcs* operons; whole-genome sequencing; carbon source utilization

Introduction

Cellulose is a polymer consisting of linear chains of β-(1→4)-linked glucose units [1, 2]. Although cellulose is the most abundant biopolymer on Earth, bacterial cellulose (BC) has attracted considerable attention due to its high purity—being free of lignin, hemicellulose, and other plant-derived components—its nanoscale structure, and its high water retention capacity [3]. Among BC-producing members of the family *Acetobacteraceae*, the genus *Komagataeibacter* stands out due to its robust cellulose biosynthetic machinery and industrial relevance [4].

BC production is strongly influenced by culture conditions, including temperature, pH and the composition of the production medium [5, 6]. Optimal temperature and pH conditions for bacterial growth may vary among strains, resulting in differences in BC production [7, 8]. The composition of the production medium, particularly the type and concentration of the carbon source, also plays an important role by affecting bacterial growth and cellulose biosynthesis [6]. In addition to the carbon source, supplementation of the production medium with compounds such as ethanol and vegetable oils has been investigated as a strategy to enhance BC production [9–12]. However, the effects of such supplements may vary depending on the bacterial strain and cultivation conditions, emphasizing the importance of strain-specific optimization of BC production.

Cellulose synthesis and secretion are mediated by a membrane-associated cellulose synthase complex that utilizes UDP-glucose as the activated glucose donor, incorporating glucose units into the growing β-1,4-glucan chain [2, 13]. BcsA and BcsB form the core cellulose synthase complex [14–16], whereas BcsC and BcsD are involved in cellulose translocation and organization, respectively [17–19]. Accessory proteins, including CcpAx/BcsH, CMCax/BcsZ, and BglAx, also contribute to cellulose biosynthesis and the organization of

the cellulose network [20–22]. In *Komagataeibacter*, the genes involved in cellulose biosynthesis are organized into cellulose biosynthesis (*bcs*) gene clusters. The main *bcs* operon comprises *bcsA*, *bcsB*, *bcsC*, and *bcsD*, and is flanked by the accessory genes *ccpAx*/*bcsH* and *cmcAx*/*bcsZ* upstream and *bglAx* downstream [16, 20, 23]. Four distinct *bcs* gene clusters with different gene organizations, including this canonical operon, have been reported in several *Komagataeibacter* species [23–26].

In a previous study, we isolated acetic acid bacteria from fruits and home-made fruit vinegars, and one isolate, GUS3, obtained from white grape vinegar, produced approximately 1 g/L BC in HS medium after 7 days of incubation [27]. Species-level identification could not be achieved using 16S rRNA and 16S–23S ITS sequencing, and the isolate was therefore designated *Komagataeibacter* sp. GUS3. In the present study, whole-genome sequencing was performed to enable species-level identification and to investigate the genomic basis of cellulose biosynthesis and carbon-source utilization. BC production by GUS3 was evaluated by examining the effects of temperature, pH, and carbon source and by assessing the effects of ethanol and oil supplementation. The resulting BC was further characterized by Fourier-transform infrared (FTIR) spectroscopy and scanning electron microscopy (SEM), as well as by determining its water-holding capacity and rehydration ratio. Overall, this study integrates genomic analysis, evaluation of the effects of cultivation conditions on BC production, and characterization of the resulting cellulose to assess the biotechnological potential of GUS3.

Materials and Methods

Strain and culture conditions

Strain GUS3, isolated from homemade grape vinegar [27], was stored at −80 °C in acetic acid medium (AAM) [28] supplemented with 20% glycerol. For revival, the strain was streaked

onto AAM agar and incubated at 25 °C for 72 h. Single colonies were then used to inoculate cellulose production media.

DNA isolation and genome sequencing

DNA preparation was performed from a 48–72 h culture grown in AAM at 25 °C with shaking at 150 rpm. Approximately 3–4 loopfuls of culture spheres (cells + cellulose pellicles) were aseptically collected and used for DNA extraction with the PureLink™ Genomic DNA Mini Kit (Thermo Scientific, Waltham, USA) with a slight modification. To disassemble the produced cellulose, the cell–pellicle mixture was homogenized in a TissueLyser (Qiagen, Hilden, Germany) with 200 mg glass beads (D = 0.5 mm) in digestion buffer for 2 min at 50 Hz, followed by 2 min on ice, repeated three times. The protocol was continued with proteinase K incubation following the manufacturer's instructions. DNA was eluted in 100 µL 10 mM Tris-HCl (pH 8.5).

DNA sequencing was performed at MicrobesNG (Birmingham, UK) using the Illumina NovaSeq platform. Illumina whole-genome shotgun sequencing generated 1,559,650 reads, of which 1,402,481 had an insert size >300 bp. Reads were trimmed using Trimmomatic [29].

Genome assembly and annotation

The Illumina whole-genome shotgun (WGS) reads of strain GUS3 have been deposited in the National Center for Biotechnology Information (NCBI) database under BioProject accession PRJNA833415, BioSample accession SAMN27988010, and WGS project accession JALQSP000000000. The genome was assembled using SPAdes v3.15.4 [30], with GenBank and RefSeq assembly accession numbers GCA_023241635.1 and GCF_023241635.1, respectively. Genome annotation was performed using the NCBI Prokaryotic Genome Annotation Pipeline (PGAP, v6.10), and the RefSeq annotation (accession GCF_023241635.1-RS_2025_12_15; released December 15, 2025) was used for downstream analyses. The circular genome map of GUS3 was generated using the Proksee platform [31].

Genome-based species identification and phylogenomic analysis

Average Nucleotide Identity based on BLAST (ANIb) between strain GUS3 and the type strains of phylogenetically related species within the genus *Komagataeibacter* was calculated using JSpeciesWS [32]. Digital DNA–DNA hybridization (dDDH) values were determined using the Genome-to-Genome Distance Calculator (GGDC) as implemented in the Type Strain Genome Server (TYGS), applying formula 2 (d4), which is recommended for draft genomes [33]. dDDH values are reported together with their 95% confidence intervals (CI). Phylogenomic relationships were inferred using TYGS. Pairwise intergenomic distances were calculated using the Genome BLAST Distance Phylogeny (GBDP) method based on whole-genome sequences, applying distance formula D5 and the GreedyWithTrimming algorithm. The resulting distance matrix was used to construct a phylogenomic tree within the TYGS pipeline.

Identification and analysis of cellulose biosynthesis genes

Cellulose biosynthesis-related genes were initially identified from the NCBI RefSeq annotation using keyword searches for “cellulose” and “bcs”. The genome sequence was additionally searched using tBLASTn to identify potential *bcs* genes not captured in the RefSeq annotation. Candidate proteins were further examined by BLASTp, conserved domain analysis, and genomic context, and the resulting annotations were manually curated and assigned appropriate gene designations.

Functional annotation and metabolic pathway reconstruction

Functional annotation and metabolic pathway reconstruction were performed using the Kyoto Encyclopedia of Genes and Genomes (KEGG) resources. The protein sequences predicted from the GUS3 genome were submitted to the KEGG Automatic Annotation Server (KAAS)

version 2.1 for assignment of KEGG Orthology (KO) identifiers using the bi-directional best hit (BBH) method [34]. The assigned KO identifiers were subsequently used for pathway reconstruction with KEGG Mapper [35]. Particular attention was given to pathways associated with central carbon metabolism and carbon-source utilization.

Bacterial cellulose production

Hestrin–Schramm (HS) medium was used as the reference medium for BC production and consisted of 20 g/L glucose (Sigma-Aldrich, St. Louis, MO, USA), 5 g/L yeast extract (Biolife, Milan, Italy), 5 g/L peptone (Merck, Darmstadt, Germany), 2.7 g/L Na_2PO_4 (Isolab, Eschau, Germany), and 1.15 g/L citric acid (Merck), with the pH adjusted to 6.0 [36].

A single colony was aseptically inoculated into 5 mL HS broth and incubated statically at 32 °C for 72 h. The resulting preculture was then transferred to 250 mL Erlenmeyer flasks containing 45 mL HS broth and incubated statically at 32 °C for 7 days [37, 38].

Effects of Cultivation Conditions on BC Production

The effects of cultivation conditions on BC production were evaluated using a one-factor-at-a-time (OFAT) approach, in which one variable was varied while the remaining conditions were kept constant. First, the effect of initial pH on BC production was evaluated at 30 °C by adjusting the pH of HS medium from 3.0 to 9.0 in 0.5-unit increments. Based on the results of the pH experiment, the effect of temperature was subsequently evaluated over the range of 24–38 °C in 2 °C increments. The selected pH and temperature conditions were then used to evaluate the effect of carbon source on BC production. Glucose, fructose, sucrose, lactose, and glycerol were individually tested at concentrations of 2, 4, and 6% (w/v) as the carbon source in HS medium.

The effect of different additives on BC production was further investigated by supplementing HS medium with ethanol, sunflower oil, corn oil, refined olive oil, raw olive oil, or canola oil

at concentrations of 1, 2, and 3%. All experiments were conducted under static conditions with two independent biological replicates for each condition.

Bacterial cellulose recovery and quantification

The BC formed was treated with 2% NaOH at 80 °C for 45 min, thoroughly washed with distilled water until a neutral pH was reached, and the wet weight was recorded [37, 39]. Subsequently, the samples were dried at 45 °C for 24 h and weighed again to determine the dry weight [40].

Fourier-transform infrared (FTIR) spectroscopy

The dried BC samples were analyzed by FTIR spectroscopy using an IRTracer-100 FTIR spectrometer (Shimadzu, Japan). Spectra were recorded over the wavenumber range of 4000–400 cm^{-1} with 32 scans [41].

Scanning electron microscopy (SEM)

The surface morphology and fibrillar structure of the produced BC were examined using a ZEISS EVO LS10 scanning electron microscope (Carl Zeiss Microscopy GmbH, Oberkochen, Germany). Following purification, the samples were lyophilized and sputter-coated with an Au/Pd alloy prior to imaging. Micrographs were acquired at an accelerating voltage of 10 kV using an SE1 detector.

Water-holding capacity and rehydration ratio

The purified BC membranes were cut into 4 × 4 cm pieces and gently blotted with filter paper to remove excess surface water. The samples were then weighed to determine the initial wet mass (M_w) [42, 43]. Subsequently, the membranes were dried at 45 °C for 24 h and weighed to determine the dry mass (M_d). For the rehydration assay, the dried BC samples were immersed in 30 mL of deionized water and incubated at room temperature for 24 h [42, 43]. Following incubation, excess surface water was gently removed with filter paper, and the

rehydrated mass (M_{wr}) was recorded. Water-holding capacity and rehydration ratio were calculated using the following equations [44]:

Water-holding capacity (%) = $[(M_w - M_d) / M_w] \times 100$

Rehydration ratio (%) = $[(M_{wr} - M_d) / (M_w - M_d)] \times 100$

Statistical analysis

Statistical analyses were performed using Python. Data were analyzed by one-way analysis of variance (ANOVA), followed by Tukey's honestly significant difference (HSD) test for multiple comparisons. All experiments were performed with two independent biological replicates (n = 2), and differences were considered statistically significant at $p < 0.05$.

Results

Genome features of GUS3

The RefSeq genome assembly of GUS3 (accession GCF_023241635.1) had a total size of 3.6 Mb, an ungapped length of 3.6 Mb, a GC content of 61.5%, and an average sequencing coverage of 206×. The assembly consisted of 75 scaffolds, with an N50 value of 345.9 kb and an L50 of 4. Genome quality assessment using CheckM (v1.2.3) indicated 100% completeness and 0.96% contamination [45]. A total of 3,387 genes were annotated, of which 3,261 were predicted to be protein-coding sequences (Fig. 1). A single rRNA operon, including 5S, 16S, and 23S rRNA genes, was identified on scaffold NZ_JALQSP010000030.1, and 50 tRNA genes were detected across the genome.

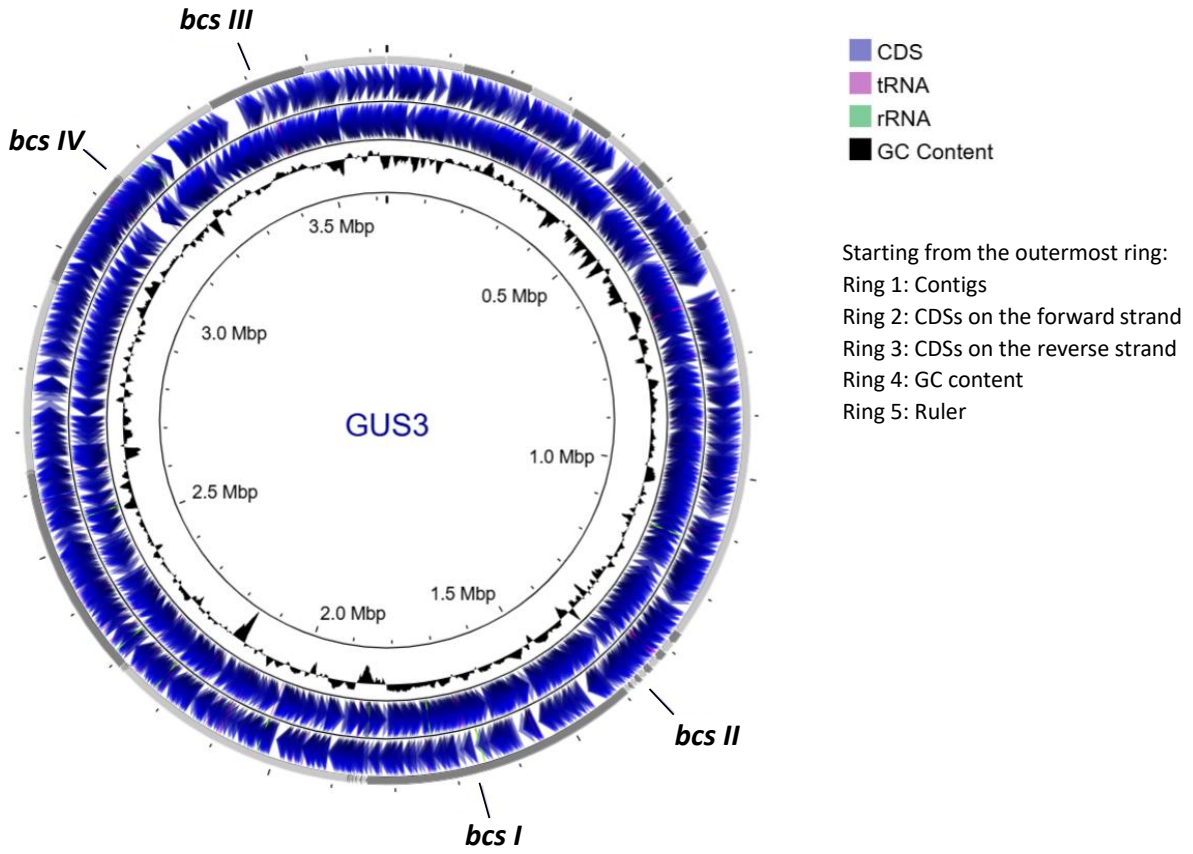


Fig. 1 Circular genome map of GUS3. The four cellulose biosynthesis gene clusters are indicated as *bcsI–bcsIV*. CDS, coding sequence.

Phylogenetic and genome-based characterization of GUS3

Genome-wide comparisons revealed that GUS3 shared 97.99% ANIb and 86.6% dDDH (95% CI: 84.0–88.9) with the type strain *K. oboediens* LMG 18849T (Table 1), supporting its identification as *K. oboediens*. Phylogenomic analysis based on whole-genome data further supported this assignment, with GUS3 clustering with the *K. oboediens* type strain and clearly separated from the type strains of other *Komagataeibacter* species (Fig. 2).

Table 1. Average Nucleotide Identity based on BLAST (ANIb) and digital DNA–DNA hybridization (dDDH) values between strain GUS3 and type species of the genus *Komagataeibacter*.

Type strain (accession number)	ANIb (%)	dDDH (%, 95% CI)
Komagataeibacter oboediens LMG 18849^T (GCF_003207815.1)	97.99	86.6 (84.0 - 88.9)
Komagataeibacter intermedius LMG 18909^T (GCF_949281285.1)	93.97	56.8 (54.0 - 59.5)
Komagataeibacter europaeus LMG 18890^T (GCF_000285295.1)	87.95	37.1 (34.7 - 39.7)
Komagataeibacter swingsii LMG 22125^T (GCF_003207895.1)	87.83	36.6 (34.1 - 39.1)
Komagataeibacter diospyri MSKU 9^T (GCF_006538165.1)	86.96	34.7 (32.3 - 37.2)
Komagataeibacter melomenusus AV436^T (GCA_013155395.1)	83.53	28.7 (26.4 - 31.2)
Komagataeibacter kakiaceti JCM 25156^T (GCA_000613305.1)	83.12	29.2 (26.8 - 31.7)
Komagataeibacter melaceti AV382^T (GCA_003403295.1)	82.73	27.5 (25.2 - 30.0)
Komagataeibacter xylinus LMG 1515^T (GCA_003207915.1)	82.93	26.9 (24.5 - 29.3)
Komagataeibacter nataicola LMG 1536^T (GCA_003207795.1)	82.69	27.2 (24.8 - 29.7)
Komagataeibacter rhaeticus LMG 22126^T (GCA_003207855.1)	82.39	26.7 (24.3 - 29.2)
Komagataeibacter medellinensis NBRC 3288^T (GCA_000182745.1)	82.33	27.2 (24.8 - 29.7)
Komagataeibacter saccharivorans LMG 1582^T (GCA_003207825.1)	81.30	25.5 (23.2 - 28.0)
Novacetimonas hansenii NBRC 14820^T (GCA_006539705.1)	75.51	20.7 (18.5 - 23.1)

ANIb: Average Nucleotide Identity based on BLAST

dDDH (CI): Digital DNA–DNA hybridization (dDDH) value obtained with formula 2 (d4), recommended for draft genomes, together with its 95% confidence interval (CI)

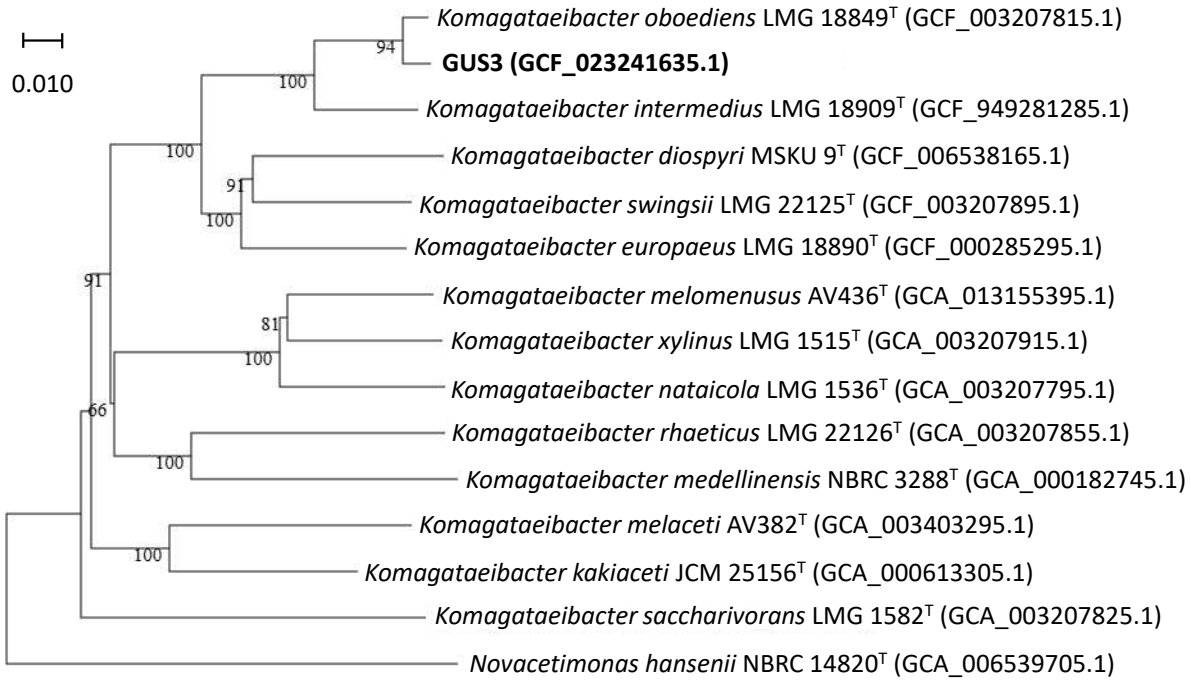


Fig. 2 Phylogenomic relationships of GUS3 within the genus *Komagataeibacter*. The tree was reconstructed based on pairwise intergenomic distances calculated according to the Genome BLAST Distance Phylogeny (GBDP) approach using the Type Strain Genome Server (TYGS). Strain GUS3 is shown in bold. *Novacetimonas hansenii* was used as an outgroup. Assembly accession numbers are shown in parentheses. Bootstrap support values are indicated at the nodes. Bar, substitutions per site.

Organization of cellulose biosynthesis (*bcs*) gene clusters in *K. oboediens* GUS3

Four cellulose biosynthesis (*bcs*) gene clusters were identified in the genome of *K. oboediens* GUS3 (Fig. 3). The canonical *bcsI* cluster comprised the *bcsA–bcsB–bcsC–bcsD* operon, flanked by *ccpAx/bcsH* and *cmcAx/bcsZ* upstream and *bglAx* downstream, whereas *bcsII* consisted of *bcsAB2–bcsX–bcsY–bcsC2*. Two additional clusters, *bcsIII* and *bcsIV*, comprised *bcsAB3–bcsC3* and a solitary *bcsAB4*, respectively. The genomic characteristics and annotations of the identified cellulose biosynthesis genes are summarized in Table 2.

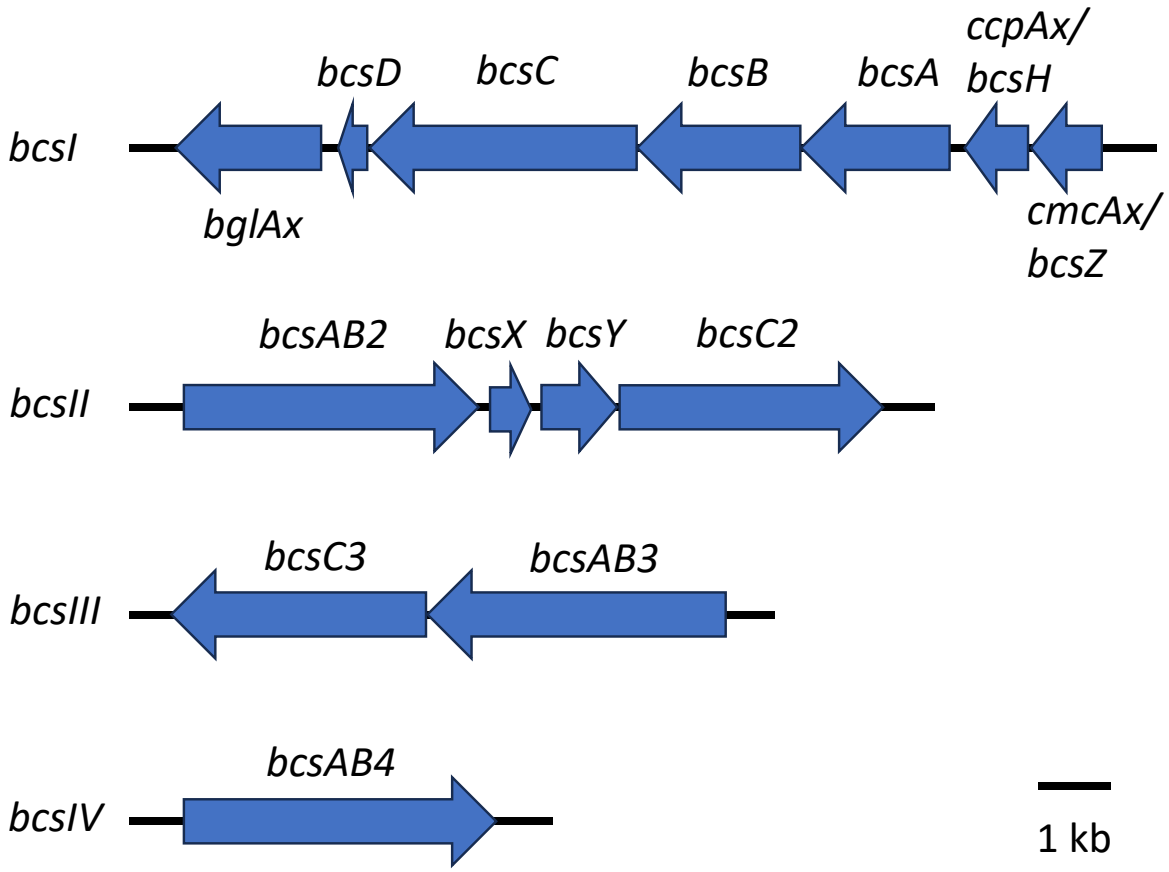


Fig. 3 Bacterial cellulose biosynthesis gene clusters identified in the genome of *Komagataeibacter oboediens* GUS3.

Tablo 2. Genomic features and annotations of cellulose biosynthesis genes identified in GUS3.

Cluster	Genomic position	Strand	Symbol	Locus tag	Protein accession
bcsI	NZ_JALQSP010000002.1: 262058-264259	-	*bglAx*	M1769_RS04230	WP_110507015.1
	NZ_JALQSP010000002.1: 264484-266954	-	*bcsD*	M1769_RS04235	WP_010513886.1
	NZ_JALQSP010000002.1: 264954-268931	-	*bcsC*	M1769_RS04240	WP_248705206.1

	NZ_JALQSP010000002.1: 268934-271363	-	*bcsB*	M1769_RS04245	WP_248705207.1
	NZ_JALQSP010000002.1: 271350-273587	-	*bcsA*	M1769_RS04250	WP_010513890.1
	NZ_JALQSP010000002.1: 273778-274785	-	*ccpAx/ bcsH*	M1769_RS04255	WP_248705208.1
	NZ_JALQSP010000002.1: 274782-275861	-	*cmcAx/ bcsZ*	M1769_RS04260	WP_214164297.1
bcsII	NZ_JALQSP010000026.1: 1-4407	+	*bcsAB2*	M1769_RS16385	WP_217320361.1
	NZ_JALQSP010000026.1: 4549-5220	+	*bcsX*	M1769_RS16390	WP_200410554.1
	NZ_JALQSP010000026.1: 5305-6465	+	*bcsY*	M1769_RS16395	WP_217320360.1
	NZ_JALQSP010000026.1: 6473-10396	+	*bcsC2*	M1769_RS16400	WP_217320359.1
bcsIII	NZ_JALQSP010000008.1: 73148-76933	-	*bcsC3*	M1769_RS11955	WP_248705343.1
	NZ_JALQSP010000008.1: 76949-81394	-	*bcsAB3*	M1769_RS11960	WP_248705344.1
bcsIV	NZ_JALQSP010000006.1: 190139-194797	+	*bcsAB4*	M1769_RS10630	WP_217319287.1

Functional annotation

KEGG Mapper reconstruction revealed a broad range of functional assignments, with KO assignments mapping to 267 KEGG pathways and 56 KEGG modules. Pathways relevant to central carbon metabolism and carbon-source utilization included glycolysis/gluconeogenesis, the pentose phosphate pathway, fructose and mannose metabolism, galactose metabolism, starch and sucrose metabolism, pyruvate metabolism, glycerolipid metabolism, and glycerophospholipid metabolism. KO assignments involved in the formation of UDP-glucose, the direct precursor of cellulose biosynthesis, included phosphoglucomutase (K01835) and UTP–glucose-1-phosphate uridylyltransferase (K00963).

Genes potentially relevant to the utilization of the carbon sources subsequently evaluated for BC production were also examined. KO assignments included oligo-1,6-glucosidase (K01182) and beta-fructofuranosidase (K01193), whereas no KO corresponding to beta-galactosidase was detected. KO assignments associated with glycerol metabolism and gluconeogenesis included glycerol kinase (K00864), glycerol-3-phosphate dehydrogenase (K00111), triosephosphate isomerase (K01803), fructose-bisphosphate aldolases (K01623 and K01624), and fructose-1,6-bisphosphatase (K11532). A detailed list of KO assignments associated with central carbon metabolism and carbon-source utilization is provided in Table S1.

BC production by *K. oboediens* GUS3

The effects of cultivation conditions on BC production were investigated using an OFAT approach, starting with the evaluation of initial medium pH (Fig. 4A). No BC production was observed at pH 8.5 or higher. Within the productive range, no significant differences in either wet or dry BC weight were observed among pH 4.5–8.0 ($p > 0.05$). Based on overall yield and experimental consistency, pH 6.5 was selected for subsequent experiments, resulting in wet and dry BC weights of 188.2 ± 14.3 g/L and 0.63 ± 0.02 g/L, respectively.

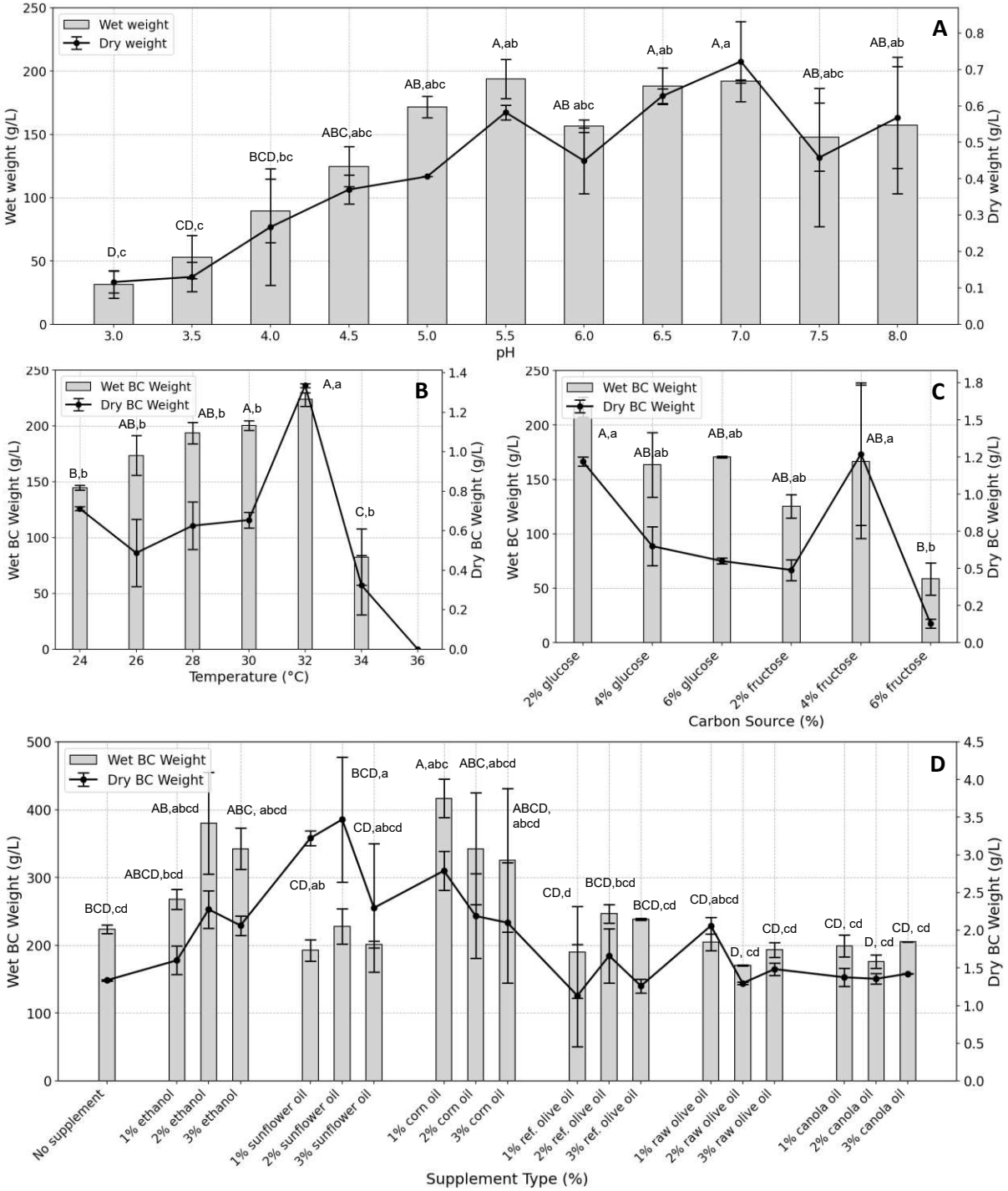


Fig. 4 Effects of culture conditions and supplementation on bacterial cellulose (BC) production by *Komagataeibacter oboediens* GUS3. (A) Effect of initial pH on BC production. (B) Effect of incubation temperature on BC production under the selected pH condition. (C) Effect of carbon source and concentration on BC production under the selected pH and temperature conditions. (D) Effect of supplementation with ethanol and vegetable oils on BC

production. Different uppercase and lowercase letters indicate significant differences in wet and dry BC weights, respectively ($p < 0.05$).

BC production was further evaluated at pH 6.5 across a wide temperature range (24–38 °C). BC formation was observed up to 34 °C; however, no cellulose was produced at 36 °C and above due to the absence of strain growth (Fig. 4B). No significant differences in wet BC weight were observed among 26, 28, 30, and 32 °C ($p > 0.05$). In contrast, dry BC weight was significantly higher at 32 °C than at all other temperatures tested ($p < 0.05$). At 32 °C, wet and dry BC weights reached 223.7 ± 6.0 g/L and 1.34 ± 0.01 g/L, respectively.

Based on the results of the pH and temperature experiments, *K. oboediens* GUS3 was further evaluated for BC production at pH 6.5 and 32 °C using different carbon sources (2–6% glucose, fructose, sucrose, lactose, and glycerol) (Fig. 4C). The strain was unable to utilize lactose, sucrose, or glycerol as carbon sources, and no BC production was detected with these substrates. No significant differences in either wet or dry BC weight were observed among 2–6% glucose and 2–4% fructose ($p > 0.05$). In contrast, 6% fructose resulted in significantly lower wet BC weight than 2% glucose and significantly lower dry BC weight than 2% glucose and 4% fructose ($p < 0.05$).

Supplementation with ethanol and vegetable oils affected both wet and dry BC production (Fig. 4D). The highest wet BC weight was obtained with 1% corn oil (416.9 ± 28.4 g/L), which was significantly higher than that of the non-supplemented control ($p < 0.05$). Although relatively high wet BC weights were also observed with 2–3% ethanol and 2–3% corn oil, these values did not differ significantly from the control ($p > 0.05$). For dry BC, the highest mean weight was obtained with 2% sunflower oil (3.47 ± 0.83 g/L), followed by 1% sunflower oil (3.22 ± 0.001 g/L). Both 1 and 2% sunflower oil resulted in significantly higher

dry BC weights than the non-supplemented control ($p < 0.05$), whereas the other supplementation conditions did not differ significantly from the control.

Characterization of BC produced by *K. oboediens* GUS3

The FTIR spectrum of BC produced by *K. oboediens* GUS3 (Fig. 5) exhibited characteristic absorption bands of cellulose. A broad band around 3345 cm^{-1} was attributed to O–H stretching, while the band around 2900 cm^{-1} corresponded to C–H stretching [46, 47]. The band observed around 1640 cm^{-1} was associated with the bending vibration of absorbed water [46]. Bands around 1430 and 1320 cm^{-1} were assigned to symmetric CH_2 bending and CH_2 wagging, respectively, while bands around 1370 and 1280 cm^{-1} were associated with C–H bending [48]. Absorption bands around 1060 and 1030 cm^{-1} were attributed to C–O stretching vibrations at the C3 and C6 positions of the glucose units, respectively[49]. Finally, the band around 900 cm^{-1} was associated with the β-(1→4)-glycosidic linkages characteristic of cellulose [46, 47].

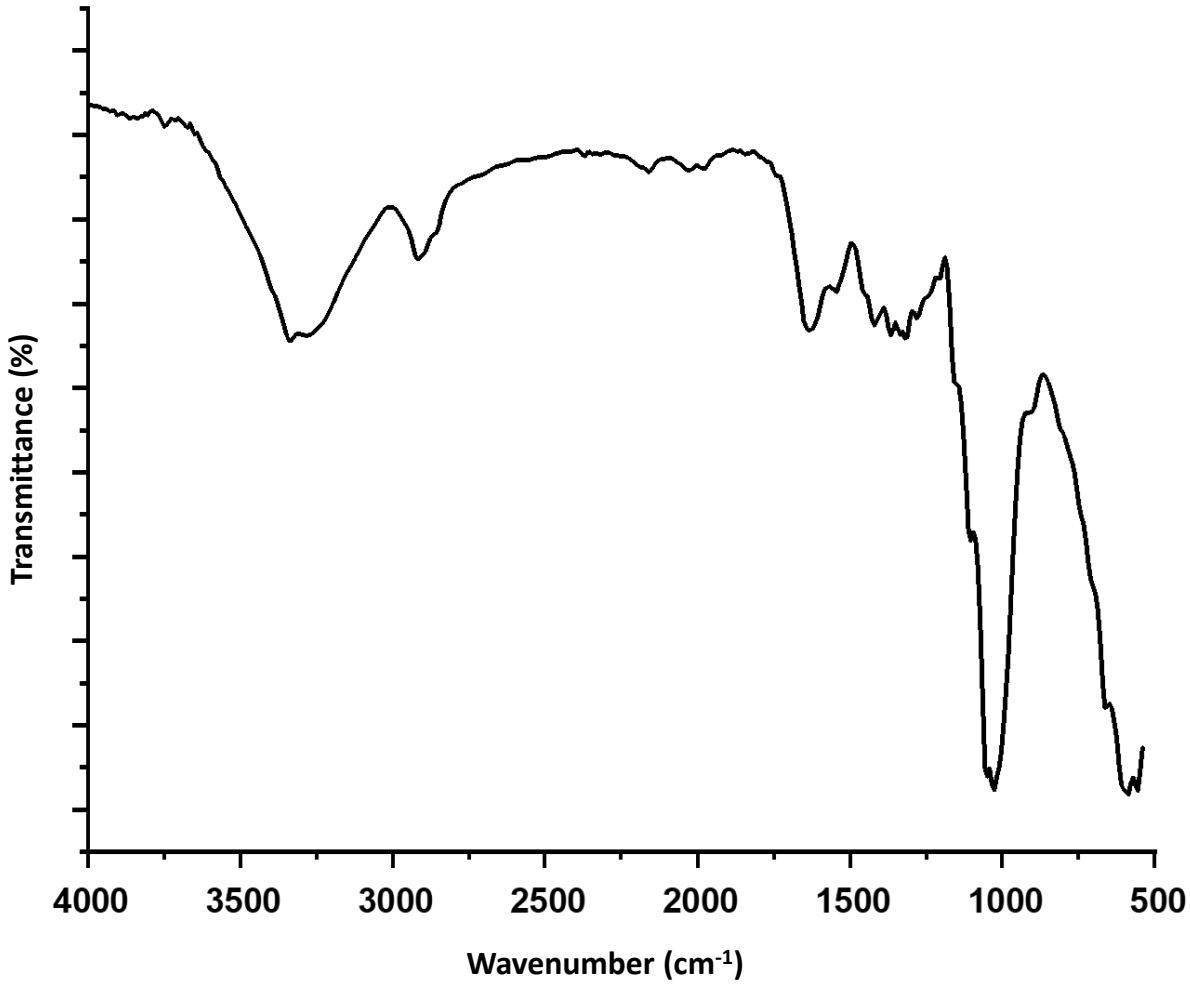


Fig. 5 Fourier-transform infrared (FTIR) spectrum of bacterial cellulose produced by *K. oboediens* GUS3.

SEM revealed a homogeneous nanofibrillar network in the lyophilized BC membrane, with fiber diameters ranging from 29 to 55 nm (Fig. 6).

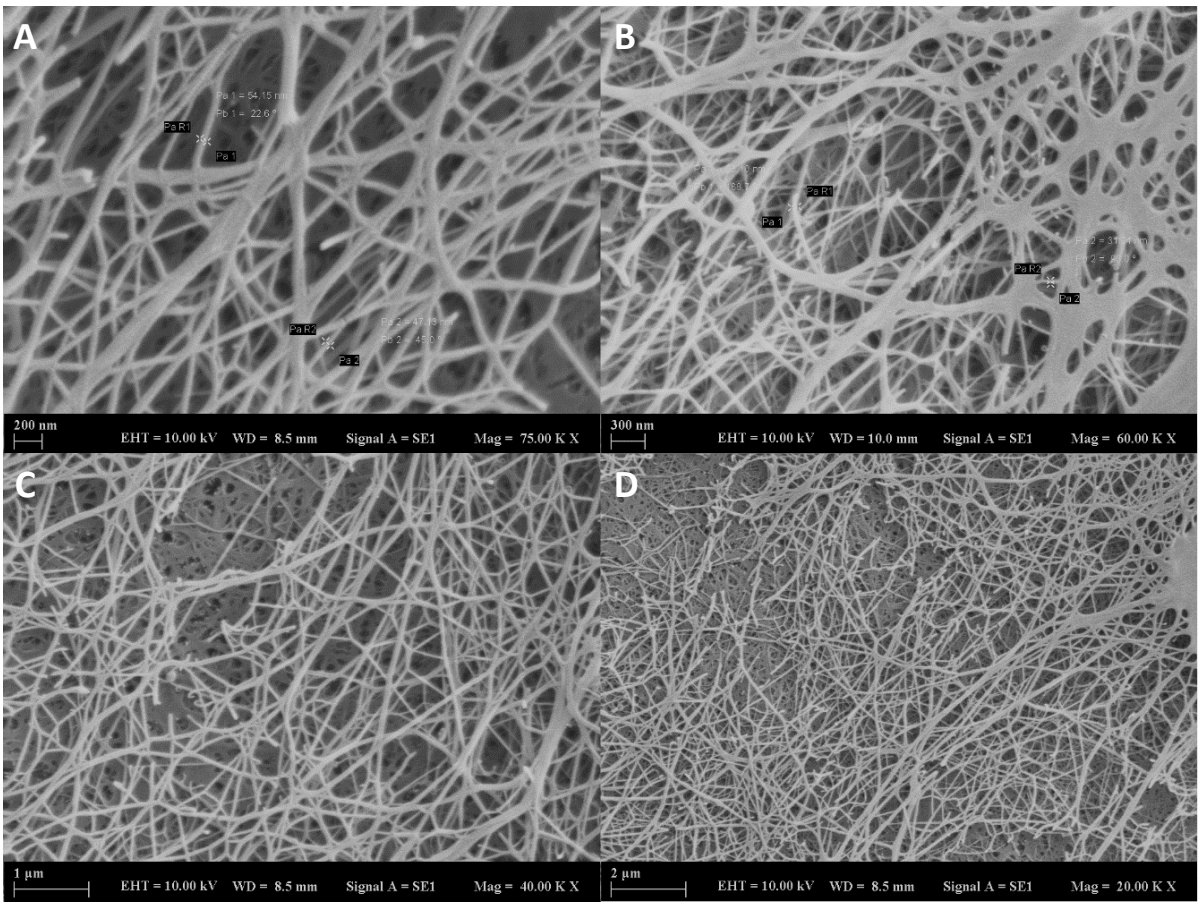


Fig. 6 Scanning electron microscopy (SEM) images of the lyophilized bacterial cellulose membrane produced by *K. oboediens* GUS3. (A) 75,000×; (B) 60,000×; (C) 40,000×; (D) 20,000× magnification. Scale bars are shown in each image.

The BC exhibited a water-holding capacity of 99.3 ± 0.035% and a rehydration ratio of 46.2 ± 6.06%.

Discussion

While previous 16S rRNA and ITS sequencing could not resolve the species-level identity of GUS3 [27], genome-wide comparisons based on ANI and dDDH, together with phylogenetic analysis, confirmed its classification as *K. oboediens*. Although the GUS3 genome was previously included in a broader pangenomic analysis [50], the present study provides a detailed characterization of its genomic features. The genome size of GUS3 (3.6 Mb) was larger than that reported for *K. oboediens* BPZTR01 (2.64 Mb) [51] but smaller than that of *K.*

oboediens KKO (3.97 Mb) [25]. The GC content of GUS3 (61.5%) was similar to that of KKO (61.4%) but lower than that of BPZTR01 (62.9%).

The organization of cellulose biosynthesis genes in *Komagataeibacter* species has been increasingly clarified through genomic studies. Four *bcs* gene clusters with a similar gene compositions and arrangements have been identified in several species, including *K. xylinus* [26], *K. medellinensis* [52], *K. rhaeticus* [25], and *K. oboediens*, although not all members of the genus possess four clusters [4]. These comprise the canonical *bcsI* cluster (*bcsA–bcsB–bcsC–bcsD*) and three additional clusters containing fused *bcsAB* genes, designated *bcsII* (*bcsAB2–bcsX–bcsY–bcsC2*), *bcsIII* (*bcsAB–bcsC3*), and *bcsIV* (*bcsAB4*) [4]. Consistent with this organization, four *bcs* gene clusters were identified in the GUS3 genome. A similar arrangement was recently reported for *K. oboediens* KKO [25].

In addition to its genomic characteristics, the BC production capacity of GUS3 was evaluated under different cultivation conditions. In the present study, no significant differences in either wet or dry BC weight were detected across the initial pH range of 4.5–8.0. However, variability between biological replicates was relatively high under some pH conditions, which may have contributed to the lack of statistically significant differences. BC production has been reported over a broad pH range, with the optimal pH varying depending on the bacterial strain and fermentation conditions. For example, BC production by *Acetobacter senegalensis* MA1 was highest at pH 4.5 [53]. Similarly, optimum pH values of 5.1 for *K xylinus* [7] and 5.5 for *Komagataeibacter rhaeticus* K23 [8] have been reported. In *K. rhaeticus* PG2, high BC production was observed at both pH 5.0 and 6.0 [54]. Higher pH values have also been reported to support BC production in some strains. For example, an optimum pH of 6.5 was reported for *Acetobacter* sp. A9, with BC production observed between pH 4.5 and 7.5 [55]. Thus, the present findings indicate that GUS3 produced BC over a relatively broad initial pH

range, although the absence of statistically significant differences does not necessarily indicate equivalent production across this range.

In addition to pH, temperature is an important factor affecting bacterial growth and BC production. In the present study, dry BC production was significantly higher at 32 °C than at all other temperatures tested, whereas no significant differences in wet BC weight were observed across the 26–32 °C range. Consistent with these findings, optimal temperatures for BC production are generally reported to fall within the 25–35 °C range, depending on the bacterial strain and cultivation conditions [6].

In the present study, no significant differences in either wet or dry BC weight were observed among 2, 4, and 6% glucose concentrations, although dry BC production tended to decrease with increasing glucose concentration. A similar concentration-dependent pattern was reported for *Komagataeibacter europaeus* 14148, where cellulose production increased from 1 to 2% glucose but decreased at concentrations of 4% and above [56]. The authors suggested that higher glucose concentrations may increase medium viscosity and bacterial growth, thereby limiting oxygen availability and reducing cellulose production. Similarly, *Komagataeibacter medellinensis* showed the highest cellulose production at 2% glucose, followed by a decrease at 3% [57]. Thus, the absence of increased BC production at higher glucose concentrations in GUS3 is consistent with previous observations in other *Komagataeibacter* strains.

When fructose was used as the carbon source, GUS3 showed the highest BC production at 4%, although the difference from 2% was not statistically significant. BC production decreased significantly at 6% fructose. Similarly, *K. medellinensis* showed the highest cellulose production at 2% fructose, with lower production at 1 and 3% [57]. Tseng et al. (2023) also reported the highest BC production at 2% fructose, followed by a decrease with increasing fructose concentration. These findings suggest that the fructose concentration

associated with maximum BC production may vary among strains, while higher concentrations may negatively affect production.

Disaccharides such as sucrose and lactose generally require hydrolysis into their constituent monosaccharides before they can enter central carbon metabolism and contribute to cellulose biosynthesis [58]. Although the GUS3 genome contained a KO assignment for beta-fructofuranosidase (K01193, Table S1), an enzyme associated with sucrose hydrolysis, no growth or BC production was observed when sucrose was supplied as the carbon source. Thus, the presence of a KO assignment associated with sucrose hydrolysis did not correspond to an observable capacity to utilize sucrose under the conditions tested. In contrast, no KO assignment corresponding to β-galactosidase, which catalyzes the hydrolysis of lactose into glucose and galactose, was detected. This may partly explain the absence of growth and BC production when lactose was used as the carbon source.

Although GUS3 did not grow or produce BC when glycerol was supplied as the carbon source, its genome contained KO assignments for several enzymes potentially involved in glycerol metabolism and gluconeogenesis. Glycerol can be phosphorylated by glycerol kinase (GlpK) to glycerol-3-phosphate and subsequently converted to dihydroxyacetone phosphate (DHAP), which can enter gluconeogenesis and contribute to UDP-glucose formation, the direct precursor of cellulose biosynthesis [58]. Consistent with this potential pathway, KO assignments corresponding to glycerol kinase (K00864), glycerol-3-phosphate dehydrogenase (K00111), triosephosphate isomerase (K01803), fructose-bisphosphate aldolases (K01623 and K01624), and fructose-1,6-bisphosphatase (K11532) were identified (Table S1). However, the presence of these assignments does not establish that glycerol can be effectively metabolized by GUS3 under the cultivation conditions tested.

The effects of vegetable oil supplementation on BC production by GUS3 differed depending on the type of oil and whether wet or dry BC weight was considered. Supplementation with

1% corn oil significantly increased wet BC weight compared with the control, whereas 1 and 2% sunflower oil significantly increased dry BC weight. A stimulatory effect of vegetable oil supplementation on BC production has previously been reported in *K. xylinus* strains, with the addition of 1% rapeseed oil increasing both wet and dry BC yields [12]. Wet BC weight reflects both cellulose accumulation and water retained within the cellulose network, whereas dry weight more directly reflects cellulose production. Therefore, the increase in wet BC weight with 1% corn oil, without a corresponding significant increase in dry weight, may partly reflect differences in water-holding capacity or cellulose structure rather than increased cellulose synthesis alone. In contrast, the increase in dry BC weight with sunflower oil provides stronger evidence of enhanced cellulose production. Further studies examining the water-holding capacity and microstructure of BC produced under different supplementation conditions could help clarify these differences.

FTIR analysis of BC produced by GUS3 revealed characteristic absorption bands of cellulose, including those associated with hydroxyl and C–H groups, C–O stretching vibrations, and β-(1→4)-glycosidic linkages, consistent with previous reports [46–49]. SEM analysis showed a homogeneous nanofibrillar network with fiber diameters ranging from 29 to 55 nm. In comparison, fiber diameters of 80–100 nm were reported for BC produced by *K. xylinus* TJU-S8 [42], while broader ranges of 30–105 nm and 20–100 nm have been reported in other studies [59, 60]. These differences in fiber dimensions may reflect variations in bacterial strains and cultivation conditions.

The BC produced by GUS3 exhibited a high water-holding capacity (99.3 ± 0.035%), comparable to previously reported values of 99.29 ± 0.23% [42] and 99.5% [59]. Its rehydration ratio was 46.2 ± 6.06%, indicating partial recovery of water after drying. The high water-holding capacity is consistent with the hydrophilic nature of cellulose and its interconnected nanofibrillar structure.

This study provides a comprehensive characterization of *K. oboediens* GUS3 by integrating genome analysis, evaluation of bacterial cellulose (BC) production under different cultivation conditions, and characterization of the resulting cellulose. Genome-wide analyses confirmed the taxonomic identity of GUS3 and revealed four cellulose biosynthesis gene clusters. BC production was influenced by cultivation conditions, with the highest dry BC production among the tested temperatures observed at 32 °C. Supplementation with 1% corn oil significantly increased wet BC weight, whereas 1 and 2% sunflower oil significantly enhanced dry BC production. Although genomic analysis identified enzymes potentially involved in sucrose and glycerol metabolism, GUS3 did not grow or produce BC when these substrates were supplied as carbon sources, highlighting the importance of evaluating genomic predictions alongside experimental observations. The BC produced by GUS3 exhibited characteristic FTIR absorption bands, a homogeneous nanofibrillar structure, and high water-holding capacity. Overall, these findings expand current knowledge of the genomic and physiological characteristics of *K. oboediens* and provide a basis for further investigations into the production and properties of BC by GUS3.

Funding

This work was supported by Istanbul Sabahattin Zaim University under Grant No. BAP-1000-42, awarded to B.M.

Author contributions

Banu Metin: Conceptualization, Methodology, Investigation, Supervision, Project administration, Funding acquisition, Writing - review & editing.

Hümeyra Odabaş: Methodology, Investigation, Formal analysis, Data curation, Visualization, Writing – original draft.

Data availability

The genome assembly of *Komagataeibacter oboediens* GUS3 is available in GenBank under accession number GCA_023241635.1 (BioProject PRJNA833415). Additional data supporting the findings of this study are available from the corresponding author upon reasonable request.

Declarations

Competing interests

The authors declare no competing interests.

Supplementary Information

Table S1. KEGG Orthology (KO) assignments associated with central carbon metabolism and carbon-source utilization in *Komagataeibacter oboediens* GUS3.

References

1. French AD (2017) Glucose, not cellobiose, is the repeating unit of cellulose and why that is important. Cellulose 24:4605–4609. https://doi.org/10.1007/s10570-017-1450-3

2. Liu M, Shen X, Guo F, et al (2026) Unraveling the biosynthesis and regulation mechanism of bacterial cellulose: Challenges and strategies toward industrial production. Carbohydr Polym 377:124891. https://doi.org/10.1016/j.carbpol.2026.124891

3. Ma L, Bi Z, Xue Y, et al (2020) Bacterial cellulose: An encouraging eco-friendly nano-candidate for energy storage and energy conversion. J Mater Chem A 8: 5812–5842. https://doi.org/10.1039/C9TA12536A

4. Brandão PR, Crespo MTB, Nascimento FX (2022) Phylogenomic and comparative analyses support the reclassification of several *Komagataeibacter* species as novel

members of the *Novacetimonas* gen. nov. and bring new insights into the evolution of cellulose synthase genes. Int. J. Syst. Evol. Microbiol. 72:005252. https://doi.org/10.1099/ijsem.0.005252

5. El-Gendi H, Taha TH, Ray JB, Saleh AK (2022) Recent advances in bacterial cellulose: a low-cost effective production media, optimization strategies and applications. Cellulose 29:7495–7533. https://doi.org/10.1007/s10570-022-04697-1

6. Fernandes I de AA, Pedro AC, Ribeiro VR, et al (2020) Bacterial cellulose: From production optimization to new applications. Int J Biol Macromol 164:2598–2611. https://doi.org/10.1016/j.ijbiomac.2020.07.255

7. Son J, Lee KH, Lee T, et al (2022) Enhanced production of bacterial cellulose from miscanthus as sustainable feedstock through statistical optimization of culture conditions. Int J Environ Res Public Health 19:866. https://doi.org/10.3390/ijerph19020866

8. Uğurel C, Öğüt H (2024) Optimization of bacterial cellulose production by *Komagataeibacter rhaeticus* K23. Fibers 12:29. https://doi.org/10.3390/fib12030029

9. Adamopoulou V, Bekatorou A, Brinias V, et al (2024) Optimization of bacterial cellulose production by *Komagataeibacter sucrofermentans* in synthetic media and agrifood side streams supplemented with organic acids and vitamins. Bioresour Technol 398:130511. https://doi.org/10.1016/j.biortech.2024.130511

10. Andriani D, Apriyana AY, Karina M (2020) The optimization of bacterial cellulose production and its applications: a review. Cellulose 27:6747–6766. https://doi.org/10.1007/s10570-020-03273-9

11. Ryngajłło M, Jacek P, Cielecka I, et al (2019) Effect of ethanol supplementation on the transcriptional landscape of bionanocellulose producer *Komagataeibacter xylinus* E25. Appl Microbiol Biotechnol 103:6673–6688. https://doi.org/10.1007/s00253-019-09904-x

12. Żywicka A, Junka AF, Szymczyk P, et al (2018) Bacterial cellulose yield increased over 500% by supplementation of medium with vegetable oil. Carbohydr Polym 199:294–303. https://doi.org/10.1016/j.carbpol.2018.06.126

13. Sumini M, Andrade GJS, Tischer CA, et al (2025) Production of bacterial cellulose by *Komagataeibacter xylinus*: biochemistry, synthesis and applications. Cellulose 32:81–94. https://doi.org/10.1007/s10570-024-06179-y

14. Morgan JLW, Strumillo J, Zimmer J (2013) Crystallographic snapshot of cellulose synthesis and membrane translocation. Nature 493:181–186. https://doi.org/10.1038/nature11744

15. Omadjela O, Narahari A, Strumillo J, et al (2013) BcsA and BcsB form the catalytically active core of bacterial cellulose synthase sufficient for in vitro cellulose synthesis. Proc Natl Acad Sci 110:17856–17861. https://doi.org/10.1073/pnas.1314063110

16. Römling U, Galperin MY (2015) Bacterial cellulose biosynthesis: Diversity of operons, subunits, products, and functions. Trends Microbiol 23:545–557. https://doi.org/10.1016/j.tim.2015.05.005

17. Acheson JF, Derewenda ZS, Zimmer J (2019) Architecture of the cellulose synthase outer membrane channel and ıts association with the periplasmic TPR domain. Structure 27:1855-1861.e3. https://doi.org/10.1016/j.str.2019.09.008

18. Hu S-Q, Gao Y-G, Tajima K, et al (2010) Structure of bacterial cellulose synthase subunit D octamer with four inner passageways. Proc Natl Acad Sci 107:17957–17961. https://doi.org/10.1073/pnas.1000601107

19. Kondo T, Nakamura Y, Nojima S, et al (2022) The BcsD subunit of type I bacterial cellulose synthase interacts dynamically with the BcsAB catalytic core complex. FEBS Lett 596:3069–3086. https://doi.org/10.1002/1873-3468.14495

20. Bimmer M, Reimer M, Klingl A, et al (2023) Analysis of cellulose synthesis in a high-producing acetic acid bacterium *Komagataeibacter hansenii*. Appl Microbiol Biotechnol 107:2947–2967. https://doi.org/10.1007/s00253-023-12461-z

21. Manan S, Ullah MW, Ul-Islam M, et al (2022) Bacterial cellulose: Molecular regulation of biosynthesis, supramolecular assembly, and tailored structural and functional properties. Prog Mater Sci 129:100972. https://doi.org/10.1016/j.pmatsci.2022.100972

22. Sunagawa N, Fujiwara T, Yoda T, et al (2013) Cellulose complementing factor (Ccp) is a new member of the cellulose synthase complex (terminal complex) in *Acetobacter xylinum*. J Biosci Bioeng 115:607–612. https://doi.org/10.1016/j.jbiosc.2012.12.021

23. Tian A, Gao H, An S, et al (2026) Targeted gene editing of bacterial cellulose biosynthesis-related genes enables programmable mechanical properties of bacterial cellulose. Bioresour Technol 446:134170. https://doi.org/10.1016/j.biortech.2026.134170

24. Deng S, Wang L, Chen G, et al (2025) Complete genome analysis of the cellulose producing strain *Komagataeibacter sucrofermentans* SMEG01. Sci Rep 15:23102. https://doi.org/10.1038/s41598-025-07045-y

25. Dias JD, Karničnik B, Nagar DN, et al (2026) Genomic characterisation of cellulose-producing *Komagataeibacter strains* KKR and KKO isolated from kombucha. Sci Rep 16:31087. https://doi.org/10.1038/s41598-026-59660-y

26. Liu M, Liu L, Jia S, et al (2018) Complete genome analysis of *Gluconacetobacter xylinus* CGMCC 2955 for elucidating bacterial cellulose biosynthesis and metabolic regulation. Sci Rep 8:6266. https://doi.org/10.1038/s41598-018-24559-w

27. Buyukduman E, Kirtil HE, Metin B (2022) Molecular ıdentification and technological properties of acetic acid bacteria ısolated from Malatya apricot and home-made fruit vinegars. Microbiol Biotechnol Lett 50:81–88. https://doi.org/10.48022/mbl.2109.09017

28. Wieme AD, Spitaels F, Aerts M, et al (2014) Effects of growth medium on matrix-assisted laser desorption–ionization time of flight mass spectra: a case study of acetic acid bacteria. Appl Environ Microbiol 80:1528–1538. https://doi.org/10.1128/AEM.03708-13

29. Bolger AM, Lohse M, Usadel B (2014) Trimmomatic: a flexible trimmer for Illumina sequence data. Bioinformatics 30:2114–2120. https://doi.org/10.1093/bioinformatics/btu170

30. Bankevich A, Nurk S, Antipov D, et al (2012) SPAdes: A new genome assembly algorithm and ıts applications to single-cell sequencing. J Comput Biol 19:455–477. https://doi.org/10.1089/cmb.2012.0021

31. Grant JR, Enns E, Marinier E, et al (2023) Proksee: in-depth characterization and visualization of bacterial genomes. Nucleic Acids Res 51:W484–W492. https://doi.org/10.1093/nar/gkad326

32. Richter M, Rosselló-Móra R, Oliver Glöckner F, Peplies J (2016) JSpeciesWS: A web server for prokaryotic species circumscription based on pairwise genome comparison. Bioinformatics 32:929–931. https://doi.org/10.1093/bioinformatics/btv681

33. Meier-Kolthoff JP, Göker M (2019) TYGS is an automated high-throughput platform for state-of-the-art genome-based taxonomy. Nat Commun 10:2182. https://doi.org/10.1038/s41467-019-10210-3

34. Moriya Y, Itoh M, Okuda S, et al (2007) KAAS: An automatic genome annotation and pathway reconstruction server. Nucleic Acids Res 35:W182–W185. https://doi.org/10.1093/nar/gkm321

35. Kanehisa M, Sato Y (2020) KEGG Mapper for inferring cellular functions from protein sequences. Protein Sci 29:28–35. https://doi.org/10.1002/pro.3711

36. Hestrin S, Schramm M (1954) Synthesis of cellulose by *Acetobacter xylinum*. II. Preparation of freeze-dried cells capable of polymerizing glucose to cellulose. Biochem J 58:345–352. https://doi.org/10.1042/bj0580345

37. Aydın YA, Aksoy ND (2014) Isolation and characterization of an efficient bacterial cellulose producer strain in agitated culture: *Gluconacetobacter hansenii* P2A. Appl Microbiol Biotechnol 98:1065–1075. https://doi.org/10.1007/s00253-013-5296-9

38. Gomes FP, Silva NHCS, Trovatti E, et al (2013) Production of bacterial cellulose by *Gluconacetobacter sacchari* using dry olive mill residue. Biomass Bioenergy 55:205–211. https://doi.org/10.1016/j.biombioe.2013.02.004

39. Son C-J, Chung S-Y, Lee J-E, Kim S-J (2002) Isolation and cultivation characteristics of *Acetobacter xylinum* KJ-1 producing bacterial cellulose in shaking cultures. J Microbiol Biotechnol 12:722–728

40. Avcioglu NH, Birben M, Seyis Bilkay I (2021) Optimization and physicochemical characterization of enhanced microbial cellulose production with a new Kombucha consortium. Process Biochem 108:60–68. https://doi.org/10.1016/j.procbio.2021.06.005

41. Revin VV, Dolganov AV, Liyaskina EV, et al (2021) Characterizing bacterial cellulose produced by *Komagataeibacter sucrofermentans* H-110 on molasses medium and obtaining a biocomposite based on it for the adsorption of fluoride. Polymers 13:1422. https://doi.org/10.3390/polym13091422

42. Du R, Zhao F, Peng Q, et al (2018) Production and characterization of bacterial cellulose produced by *Gluconacetobacter xylinus* isolated from Chinese persimmon vinegar. Carbohydr Polym 194:200–207. https://doi.org/10.1016/j.carbpol.2018.04.041

43. Wang J, Tavakoli J, Tang Y (2019) Bacterial cellulose production, properties and applications with different culture methods – A review. Carbohydr Polym 219:63–76. https://doi.org/10.1016/j.carbpol.2019.05.008

44. Zhang W, Wang X, Qi X, et al (2018) Isolation and identification of a bacterial cellulose synthesizing strain from kombucha in different conditions: *Gluconacetobacter xylinus* ZHCJ618. Food Sci Biotechnol 27:705–713. https://doi.org/10.1007/s10068-018-0303-7

45. Parks DH, Imelfort M, Skennerton CT, et al (2015) CheckM: assessing the quality of microbial genomes recovered from isolates, single cells, and metagenomes. Genome Res 25:1043–1055. https://doi.org/10.1101/gr.186072.114

46. Abol-Fotouh D, Hassan MA, Shokry H, et al (2020) Bacterial nanocellulose from agro-industrial wastes: low-cost and enhanced production by *Komagataeibacter saccharivorans* MD1. Sci Rep 10:3491. https://doi.org/10.1038/s41598-020-60315-9

47. Li Z-Y, Azi F, Ge Z-W, et al (2021) Bio-conversion of kitchen waste into bacterial cellulose using a new multiple carbon utilizing *Komagataeibacter rhaeticus*: Fermentation profiles and genome-wide analysis. Int J Biol Macromol 191:211–221. https://doi.org/10.1016/j.ijbiomac.2021.09.077

48. Sun Y, Lin L, Haibo D, et al (2008) Structural changes of bamboo cellulose in formic acid. BioResources 3:297–315. https://doi.org/10.15376/biores.3.2.297-315

49. Jeoh T, Nill JD, Zhao W, et al (2024) Spatiotemporal dynamics of cellulose during enzymatic hydrolysis studied by infrared spectromicroscopy. Green Chem 26:396–411. https://doi.org/10.1039/d3gc03279e

50. Akhoon BA, Qiao Q, Stewart A, et al (2025) Pangenomic analysis of the bacterial cellulose-producing genera *Komagataeibacter* and *Novacetimonas*. Int J Biol Macromol 298:139980. https://doi.org/10.1016/j.ijbiomac.2025.139980

51. Pinar O, Bozdağ G, Yemişer İ, et al (2020) Complete genome sequence of a cellulose-producing bacteria Komagataeibacter oboediens BPZTR01. Genet Appl 4:38–40. https://doi.org/10.31383/ga.vol4iss1pp38-40

52. Hernández-Arriaga AM, del Cerro C, Urbina L, et al (2019) Genome sequence and characterization of the bcs clusters for the production of nanocellulose from the low pH resistant strain *Komagataeibacter medellinensis* ID13488. Microb Biotechnol 12:620–632. https://doi.org/10.1111/1751-7915.13376

53. Aswini K, Gopal NO, Uthandi S (2020) Optimized culture conditions for bacterial cellulose production by *Acetobacter senegalensis* MA1. BMC Biotechnol 20:46. https://doi.org/10.1186/s12896-020-00639-6

54. Thorat M, Dastager S (2018) High yield production of cellulose by a *Komagataeibacter rhaeticus* PG2 strain isolated from pomegranate as a new host. RSC Adv 8:29797–29805. https://doi.org/10.1039/C8RA05295F

55. Son H-J, Heo M-S, Kim Y-G, Lee S-J (2001) Optimization of fermentation conditions for the production of bacterial cellulose by a newly isolated *Acetobacter*. Biotechnol Appl Biochem 33:1–5. https://doi.org/10.1042/BA20000065

56. Tseng YS, Patel AK, Chen C-W, et al (2023) Improved production of bacterial cellulose by *Komagataeibacter europaeus* employing fruit extract as carbon source. J Food Sci Technol 60:1054–1064. https://doi.org/10.1007/s13197-022-05451-y

57. Molina-Ramírez C, Castro M, Osorio M, et al (2017) Effect of different carbon sources on bacterial nanocellulose production and structure using the low ph resistant strain *Komagataeibacter medellinensis*. Materials 10:639. https://doi.org/10.3390/ma10060639

58. Zikmanis P, Kolesovs S, Ruklisha M, Semjonovs P (2021) Production of bacterial cellulose from glycerol: the current state and perspectives. Bioresour Bioprocess 8:116. https://doi.org/10.1186/s40643-021-00468-1

59. Gupta A, Keddie DJ, Kannappan V, et al (2019) Production and characterisation of bacterial cellulose hydrogels loaded with curcumin encapsulated in cyclodextrins as wound dressings. Eur Polym J 118:437–450. https://doi.org/10.1016/j.eurpolymj.2019.06.018

60. Ramírez Tapias YA, Di Monte MV, Peltzer MA, Salvay AG (2022) Bacterial cellulose films production by Kombucha symbiotic community cultured on different herbal infusions. Food Chem 372:131346. https://doi.org/10.1016/j.foodchem.2021.131346